# Accepted Manuscript

Title: Enhancing the photocatalytic activity of GaN by electrochemical etching

Author: Dezhong Cao Hongdi Xiao Hangzhou Xu Jishi Cui Qingxue Gao Haiyan Pei

# Enhancing the photocatalytic activity of GaN by electrochemical etching

Dezhong Cao[a], Hongdi Xiao[a*]hdxiao@sdu.edu.cn, Hangzhou Xu[b], Jishi Cui[a],Qingxue Gao[a],

Haiyan Pei[b]

[a]School of Physics, Shandong University, Jinan 250100, People's Republic of China.
[b]School of Environmental Science and Engineering, Shandong University, Jinan 250100, People's Republic of China

[*]Corresponding author. Tel./fax:+86 531 88377032.

**Graphical abstract**
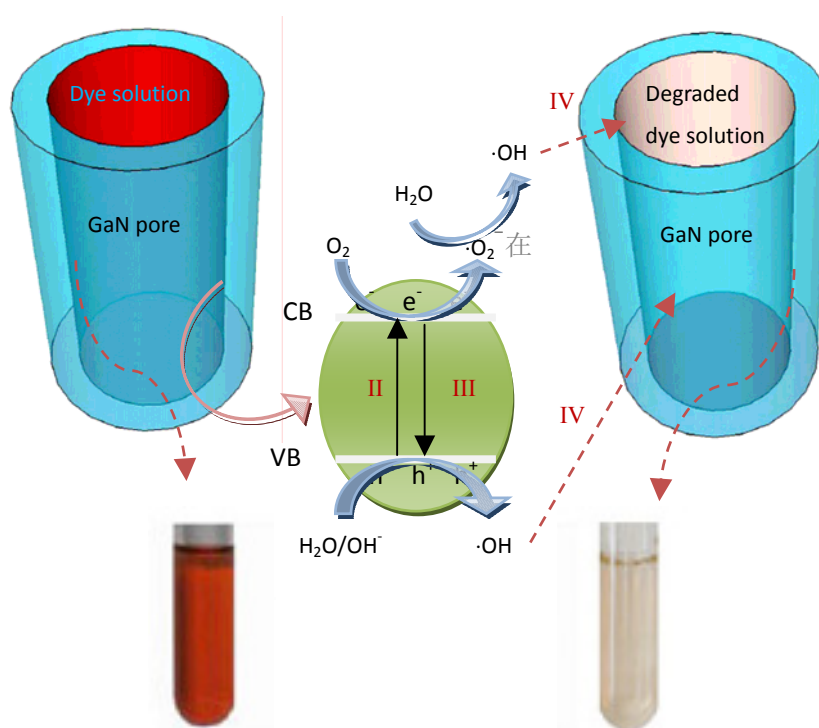


Nanoporous (NP) GaN thin films prepared via electrochemical etching method were first investigated as photocatalysts. The nanostructures exhibited excellent stability and good photocatalytic activity in dye photodegradation.

2

**Highligts**

Nanoporous (NP) GaN thin films showed better photocatalytic activity than GaN thin films.

NP GaN exhibited good ability to photodegrade organic dye at various pHs.

NP GaN had much better photocatalytic activity and more excellent stability than porous Si.

Abstract

Nanoporous (NP) GaN thin films prepared with electrochemical etching method were investigated as photocatalysts in dye photodegradation systematically. The comparison of NP GaN thin films with GaN thin films showed that NP GaN thin films with high surface-to-volume ratio exhibited much better photocatalytic activity. In comparison with porous Si wafers, NP GaN thin films with lower surface area exhibited much better photocatalytic activity, because GaN is efficient not only for dye reduction like Si, but also for dye oxidation. Due to its ceramic-like chemical inertness, moreover, NP GaN showed more excellent stability to photodegrade organic dye than porous Si under basic conditions. The band gap of GaN can be modulated in visible-light region, which will be beneficial to a photodegradation system with concentrated solar light.

4

## 1. Introduction

Research on porous semiconductors has drawn much attention, since the discovery of intense luminescence from porous Si [1, 2]. The high surface area, band gap shift, and efficient luminescence suggest uses of porous semiconductors over a wide range extending from optoelectronics to chemical and biochemical sensors applications. Another attractive application of porous semiconductor materials is in environmental remediation and hydrogen production because their high surface-to-volume (S/V) ratio results in enhanced photocatalytic effect [3]. Porous nanostructure fabricated via an electrochemical etching process is generally adhered to a rigid substrate so that this nanostructure can be easily recycled and reused in environmental remediation and hydrogen production. Nowadays, porous Si has attracted much interest because of its potential in utilizing solar energy to degrade organic pollutants [4, 5]. However, chemical properties of porous Si are unstable under harsh conditions such as low and high pH, which limits its application.

GaN is a well-known wide band-gap semiconductor that has a bandgap energy of 3.4 eV at room temperature. The conduction band minimum ($E_{CBM}$) of GaN is higher than that of $E^o(OH\cdot/OH^-)$ (-0.28 versus NHE), whereas the valence band minimums ($E_{VBM}$) of GaN is lower than that of $E^o(O_2/O_2^{\cdot-})$ (2.27 V versus NHE) [6, 7]. Based on such a realization, GaN has been used to split water for the generation of hydrogen gas and decompose organic pollutants into harmless compounds such as carbon dioxide and water [8, 9]. Due to the ceramic-like chemical inertness, moreover, it has exhibited much better stability than semiconductors based on metal oxides, such as ZnO and $TiO_2$, under acidic conditions [9]. Most important of all, the band gap

5

tunability by alloying with InN allows efficient absorption of solar spectrum. Therefore, NP GaN should be intriguing as a photocatalytic material because of its simple fabrication step as well as expected advantages of GaN nanostructures in photodegradation for organic pollutants.

In this study, we reported the fabrication of NP GaN thin films by electrochemical etching in HF solution, and its photocatalytic activity for direct fast scarlet 4BS dye was characterized. In comparison with porous Si wafers, NP GaN thin films exhibited more excellent chemical stability, and much better photocatalytic efficiency. It implied that NP GaN and its alloys are promising photocatalytic materials under concentrated solar light intensity.
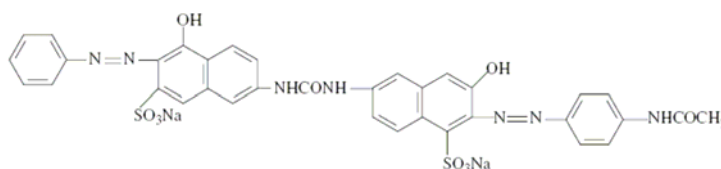
## 2. Experimental

### 2.1 Fabrication of NP GaN thin films

Electrochemical (EC) porosification experiments were conducted in a two-electrode cell at room temperature with n-type GaN (0002) thin films or n-type Si (100) wafers (the resistivity of 0.5-1 $\Omega$ cm) as the anode and a platinum wire as the counter electrode (cathode) [10, 11]. The structure of n-type GaN films is that Ga-polar Si doped GaN of 2 $\mu m$ thickness was grown on c-plane sapphire with undoped GaN layer of 500 nm used as an etch stop by metal-organic chemical vapor deposition (MOCVD) with a doping density of $8 \times 10^{18}$ cm$^{-3}$ [12]. The electrolytes were prepared by adding ethanol to HF (49%) with a volume ratio of 1:1. The anodization process was carried out in a potentiostatic (constant voltage) mode controlled by a Gwinstek GPD-3303S source meter. After anodization, samples were rinsed with deionized water and dried in N$_2$. Morphology of the samples was characterized with atomic force microscope (AFM) (NanoScope ⅢA) and scanning electron microscope (SEM) (Hitachi SU-70). Photoluminescence (PL) spectroscopy measurements with a He-Cd laser emitting at 325 nm were performed to identify the

6

optical characteristics of NP GaN thin films.

## 2.2 Evaluation of the photocatalytic activity

The molecule structure of direct fast scarlet 4BS (>90% purity) is shown in the following [13].



There are N=N double bonds which are chromophoric group, phenyl rings and naphthyl rings in the structure of 4BS dye. The corresponding UV-Vis absorption peaks are centered at ~498, ~334 and ~208 nm, respectively.

The photocatalytic experiments were carried out with the NP GaN films and the porous Si wafers with the area of 1 cm$^2$ in a 4 ml 4BS dye solution in a sealed quartz tube, under stirring. The initial concentration of 4BS dye solution was about $1.5\times10^{-5}$ mol L$^{-1}$. The reaction system was irradiated under ultraviolet light using a 30 W Hg lamp ($\lambda > 254$ nm). The concentration of 4BS dye was determined by UV-Vis spectrophotometer (UV-2450, Shimadzu, Japan). All of the photocatalytic reactions were carried out under air ambient and at room temperature.

## 3. Results and discussion

### 3.1 Characterization of NP GaN thin films

To evaluate the morphology and structure of NP GaN thin films prepared via the EC etching technique at 5, 10, 30 and 50 V for 1 min, SEM and AFM measurements were performed. Figs. 1(a)-1(d) show the top view SEM images of the NP GaN films. The SEM image shown in Fig. 1(a) indicates that the applied bias of 5 V is not sufficient to induce local breakdown which leads to the pore formation [14]. The root-mean-square (rms) roughness of the film surface measured on a 3×3

7

μm area, using AFM, is 6 nm. By increasing the applied biases from 10 to 50 V, the density and diameter of GaN nanopores vary from $1.44 \times 10^{10}$ /cm$^2$ to $4.9 \times 10^{10}$ /cm$^2$, and from 17.5 nm to 35 nm, respectively (Table 1). The variations are ascribed to a stronger electric field that initiates more avalanche breakdown events per unit time [15].

Figs. 1(e)-1(h) show the cross-sectional images of the corresponding left samples. In Fig. 1(f), the etching depth along the [000$\bar{1}$] direction is about 100 nm at 10 V. At 30 and 50 V, the nanopores with approximate 2 μm in length are uniform, straight and vertical to the substrate surface, indicating that the etching rate depends on the applied bias. The trajectory of the pore can be considered as a mapping of the electric field/carrier flow contours, so a higher applied bias reflects a higher carrier rate which leads to a higher etching rate [16].

Fig. 2 displays the room-temperature PL spectra of NP GaN samples fabricated under the different applied biases. The NP GaN samples obtained at high applied bias are observed to be red-shifted relative to the samples fabricated at low applied bias. The red-shifted can be attributed to the relaxation of the compressive stress in the porous samples, which can be further confirmed by Raman scattering [17] and X-ray diffraction [18]. On the other hand, the PL intensity for the etched samples are found to be increased, which could mainly be attributed to the enhancement of the photon extraction efficiency due to more photons scattering from the sidewalls of the NP GaN [19].

## 3.2 Photocatalytic activity of NP GaN thin films

The photocatalytic activity of GaN thin films etched at the different applied biases was compared by measuring the amount of dye solutions photodegraded by the etched GaN films under UV light illumination. Figs. 3(a) and 3(b) show the removal amount of 4BS under different

8

irradiation times and the absorption spectra of 4BS solutions degraded for 8 h, respectively. After

8 h of UV illumination, the amount of organic dye degraded by GaN samples increases from 26%

to 57% with pore density rising from 0 to $4.9 \times 10^{10}$ /cm$^2$, whereas the linear increases of

removal amount indicate that the prolonged photodegraded times can lead to further increase of

removal amount (see Fig. 3(a)). The high photocatalytic activity of NP GaN thin films obtained at

50 V presumably results from the high S/V ratio of GaN nanopores.

The process of photodegradation can be roughly divided into four different stages (Fig. 4)

[7]. Stage I is photoexcitation in the nanopores, at which electron-hole pairs are created by UV

light illumination (with photo energy greater than the bandgap energy, $E_g$), transforming the

catalyst into the photoexcited state (eqn. 1). Stage II is that the electron-hole pairs are separated

and subsequently transferred to their sites on the internal surface of GaN nanopores. In parallel to

stage II, stage III is charge recombination, where a fraction of photogenerated electrons and holes

radiatively or nonradiatively recombine, or are trapped by the defects on the internal surface of

GaN nanopores. Stage IV is the redox reaction, at which further react with adsorbed water and

dissolved oxygen to produce $\cdot OH$ radicals (eqns. 2-7) which are strong and nonselective

oxidizing agents for organic pollutants. Finally, 4BS molecules are oxidized and decomposed by

the $\cdot OH$ radicals (eqn. 8).

$$GaN \xrightarrow{h\nu} h^+ + e^- \tag{1}$$

$$h^+ + H_2O \rightarrow \cdot OH + H^+, \tag{2}$$

$$h^+ + OH^- \rightarrow \cdot OH \tag{3}$$

$$e^- + O_2 \rightarrow \cdot O_2^-, \tag{4}$$

9

$$\cdot O_2^- + H^+ \to \cdot OOH \tag{5}$$

$$e^- + \cdot OOH + H^+ \to H_2O_2 \tag{6}$$

$$H_2O_2 + e^- \to \cdot OH + OH^- \tag{7}$$

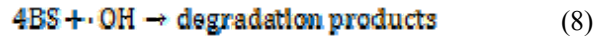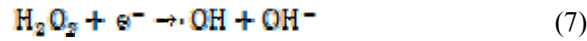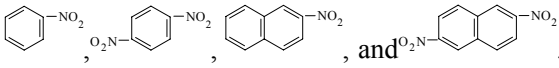$$4BS + \cdot OH \to \text{degradation products} \tag{8}$$

Fig. 5 shows the dependence of photocatalytic activity of NP GaN thin films obtained at 50 V in acidic and basic solutions. The amount of photodegraded dye in acidic solutions with pH of 2.0, 3.0, and 5.0 is 78, 82, and 70 %, respectively, whereas the amount in pH 9 solution is 41%. This indicates that the photocatalytic activity of NP GaN is more effective under acidic than basic conditions. Under the acidic conditions, it is easy to form N-H groups on the internal surface of GaN nanopores, so this pH dependence of the photocatalytic reaction may result from a sequence of proton-transfer events from the N-H groups to the nearby OH groups and bulk water molecules [20].

We investigated the changes in surface morphology and crystal structure of NP GaN thin films obtained at 50 V using SEM (Fig. 6) and XRD (Fig. 7) before and after photodegradation at pH 2. As shown in Figs. 6 and 7, there are no apparent changes in surface morphology and diffraction peaks, which can be also observed under basic conditions. Therefore, these results indicate that NP GaN has stability to photodegrade organic dye under strong acidic or basic conditions, which is in agreement with the photocatalytic stability of GaN nanowires [9].

**3.3 Comparison of the photocatalytic activity of NP GaN with that of porous Si**

The photocatalytic activity of NP GaN thin films was compared with that of porous Si wafers because porous Si wafers have exhibited a very strong photocatalytic activity for some organic pollutants such as methyl red (MR), phenol, and methyl orange (MO) [4, 5, 21]. Porous Si (100)

10

wafers were fabricated via the EC etching technique at 15 V for 10 min. Fig. 8 shows the typical top-view and cross-sectional SEM images of porous Si with a diameter of averagely 300 nm, a pore density of $7.9 \times 10^9$/cm$^2$, and a pore depth of 60 μm. For the porous Si with the area of 1 cm$^2$, its internal surface area is larger than that of NP GaN obtained at 50 V. We measured the absorption spectra of 4BS dye solutions photodegraded by the NP GaN and the porous Si. Our observations clearly show that (i) NP GaN exhibits 57% potodegradation of chromophoric structure (λ=494 nm) of organic dye, whereas porous Si photodegrades only 33% of the dye (Fig. 9); (ii) the naphthalene and benzene rings can be photodegraded by NP GaN thin films, but absorbance of aromatic rings in 4BS solutions degraded by porous Si exhibits significant increase (Fig. 9), which may be explained by the formation of intermediate products such as


, , , and. These intermediate products have much bigger absorbency than those in the original azo dye molecules [22].

To evaluate presumably photodegradation mechanisms of NP GaN and porous Si, band levels of GaN and Si are shown in Fig. 10. The $E_{CBM}$ values of GaN and Si are higher than that of $E^o$(OH•/OH$^-$), whereas the $E_{VBM}$ value of GaN is lower than that of $E^o$(O$_2$/O$_2^{•-}$) [6, 7]. Porous Si has higher band-gap energy (1.7-1.9 eV) than bulk Si (1.1 eV) [23], but its $E_{VBM}$ value is still higher than that of $E^o$(O$_2$/O$_2^{•-}$). Therefore, GaN is efficient not only for dye reduction like Si (eqns. 4-8), but also for dye oxidation (eqns. 2, 3 and 8). Furthermore, after the photodegradation experiment under the basic condition, there is no significant change in the surface morphology of NP GaN, whereas the porous Si layers are dissolved, indicating that NP GaN has more excellent stability than porous Si.

## 4. Conclusions

11

In summary, the photocatalytic activity of NP GaN thin films was investigated for the use of NP GaN thin films as photocatalysts in harsh environments. NP GaN thin flims exhibited higher photocatalytic activity than GaN thin films because of their larger surface area, which enhanced hole transport from photocatalyst to dye solution. Furthermore, NP GaN showed higher efficiency and stability than porous Si due to its large band gap energy and ceramic-like chemical inertness. This behavior would be beneficial to a photodegradation system with concentrated solar light.

12

**References**

[1] L. T. Canham, Silicon quantum wire array fabrication by electrochemical and chemical dissolution of wafers, Appl. Phys. Lett. 57 (1990) 1046-1048

[2] V. Lehmann, U. Gosele, Porous silicon formation: A quantum wire effect, Appl. Phys. Lett. 58 (1991) 856-858

[3] D. Beytdoun, R. Amal, G. Low, S. McEvoy, Role of Nanoparticles in Photocatalysis, J. nanoparticles Res. 1 (1999) 439-458

[4] F. Y. Wang, Q. D. Yang, G. Xu, N. Y. Lei Y. K. Tsang, N. B. Wong, J. C. Ho, Highly active and enhanced photocatalytic silicon nanowire arrays, Nanoscale, 3 (2011) 3269-3276

[5] J. Y. Su, H. T. Yu, X. Quan, S. Chen, H. Wang, Hierarchically porous silicon with significantly improved photocatalytic oxidation capability for phenol degradation, Appl. Catal. B-Environ. 138 (2013) 427-433

[6] M. D. Hernández-Alonso, F. Fresno, S. Suárez, M. M. Coronado, Development of alternative photocatalysts to TiO2: Challenges and opportunities, Energy Environ. Sci. 2 (2009)1231-1257

[7] H. L. Zhou, Y. Q. Qu, T. Zeid, X. F. Duan, Towards highly efficient photocatalysts using semiconductor nanoarchitectures, Energy Environ. Sci. 5 (2012) 6732-6743

[8] S. W. Ryu, Y. Zhang, B. J. Leung, C. Yerino, J. Han, Improved photoelectrochemical water splitting efficiency of nanoporous GaN photoanode, Semicond. Sci. Tech. 27 (2012) 015014

[9] H. S. Jung, Y. J. Hong, Y. R. Li, J. H. Cho, Y. J. Kim, G. C. Yi, Photocatalysis Using GaN Nanowires, ACS Nano, 2 (2008) 637-642

[10] H. Hartono, C. B. Soh, S. Y. Chow, S.J. Chua, E. A. Fitzgerald, Reduction of threading

dislocation density in GaN grown on strain relaxed nanoporous GaN template, Appl. Phys. Lett. 90 (2007) 171917

[11] V. P. Parkhutik, V. I. Shershulsky, Theoretical modelling of porous oxide growth on aluminium, J. Phys. D: Appl. Phys. 25 (1992) 1258-1263

[12] J. Han, T. B. Ng, R. M. Biefield . M. H. Crawford, D. M. Follstaedt, The effect of $H_2$ on morphology evolution during GaN metalorganic chemical vapor deposition, Appl. Phys. Lett. 71 (1997) 3114-3116

[13] H. D. Xiao, H. Y. Pei, J. Q. Liu, J. S. Cui, B. Jiang, Q. J. Hou, W. R. Hu, Fabrication, characterization, and photocatalysis of GaN-$Ga_2O_3$ core-shell nanoparticles, Mater. Lett. 71 (2012) 145-147

[14] S. Nakamura, S. J. Pearton, G. Fasol, The Blue Laser Diode: The Complete Story (Springer, New York, 2000)

[15] M. J. Schwab, D. Chen, J. Han, L. D. Pfefferle, Aligned Mesopore Arrays in GaN by Anodic Etching and Photoelectrochemical Surface Etching, J. Phys. Chem. C 117 (2013) 16890-16895

[16] D. Chen, H. Xiao, J. Han, Nanopores in GaN by electrochemical anodization in hydrofluoric acid: Formation and mechanism, *J. Appl. Phys.* **112** (2012) 064303

[17] H. D. Xiao, J. S. Cui, D. Z. Cao, Q. X. Gao, J. Q. Liu, J. Ma, Self-standing nanoporous GaN membranes fabricated by UV-asisted electrochemical anodizaiton, Mater. Lett. 145 (2015) 304

[18] J. S. Cui, H. D. Xiao, D. Z. Cao, Z. W. Ji, I. Ma, Porosity-induced relaxation of strains at different depth of nanoporous GaN studied using the Z-scan of Raman spectroscopy, J. Alloy Comp. 626 (2015) 154

[19] A. P. Vajpeyi, S. J. Chua, S. Tripathy, E. A. Fitzgerald, W. Liu, P. Chen, L. S. Wang, High

optical quality nanoporous GaN prepared by photoelectrochemical etching, Electrochem. Solid-State Lett. 8, (2005) G85

[20] A. V. Akimov, J. T. Muckerman, O. V. Prezhdo, Nonadiabatic Dynamics of Positive Charge during Photocatalytic Water Splitting on GaN(10-10) Surface: Charge Localization Governs Splitting Efficiency, J. Am. Chem. Soc. 135 (2013) 8682

[21] H. Z. Xu, H. D. Xiao, H. Y. Pei, J. S. Cui, W. R. Hu, Photodegradation activity and stability of porous silicon wafers with (100) and (111) oriented crystal planes, Micropor. Mesopor. Mat. 204 (2015) 251

[22] J. Wang, R. Li, Z. Zhang, W. Sun, R. Xu, Y. Xie, Efficient photocatalytic degradation of organic dyes over titanium dioxide coating up conversion luminescence agent under visible and sunlight irradiation, Appl. Catal. A 334 (2008) 227-233

[23] M. A. Tischler, R. T. Collins, J. H. Stathis, and J. C. Tsang, Luminescence degradation in porous silicon, Appl. Phys. Lett. 60,639 (1992).

**Figure captions**

Fig. 1. Plan-view SEM images of GaN samples obtained by the EC etching process at (a) 5 V, (b) 10 V, (c) 30 V and (d) 50 V. (e)-(f) show cross-sectional view of the corresponding left images.

Fig. 2. PL spectra of nanoporous GaN fabricated at the different applied biases.

Fig. 3. (a) Removal amount of 4BS by the etched GaN samples under the different irradiation times. (b) Absorption spectra of 4BS solution photodegraded by the etched GaN samples for 8 h.

Fig. 4. Schematic illustrating the mechanism for photocatalytic process in GaN nanopores. (I) photoexcitation in the nanopores, (II) charge separation and transportation, (III) charge recombination in parallel to stage II, and (IV) photoassisted redox reaction.

Fig. 5. Amount of 4BS photodegraded by NP GaN at 50 V under various pHs.

Fig. 6. SEM images of NP GaN obtained at 50 V (a) before the photocatalytic reaction and (b) after the reaction at pH 2 for 8 h.

Fig. 7. XRD patterns of NP GaN obtained at 50 V before and after the photocatalytic reaction at pH 2 for 8 h.

Fig. 8. (a) Plan-view and (b) cross-sectional SEM images of porous Si fabricated by the EC etching process at 15 V.

Fig. 9. Absorption spectra of 4BS solution photodegraded by porous Si and NP GaN.

Fig. 10. Band gaps (eV) and redox potentials of GaN and Si using the normal hydrogen electrode (NHE) as a reference [ 6, 7]. This figure can't indicate that the $E_{CBM}$ of NP GaN is higher or lower than that of porous Si.

16

**Tables**

Table 1 Comparison of pore density, pore diameter, and photocatalytic activity of GaN samples

obtained at the different conditions

| samples[a] | applied bias (V) | rms surface roughness[b] (nm) | pore density ($cm^{-2}$) | pore diameter (nm) |
|:---:|:---:|:---:|:---:|:---:|
| Control | - | - | - | - |
| a | 5 | 6 | 0 | 0 |
| b | 10 | - | $1.4 \times 10^{10}$ | 17 |
| c | 30 | - | $4.7 \times 10^{10}$ | 24 |
| d | 50 | - | $4.9 \times 10^{10}$ | 35 |

[a] Corresponds to samples in Fig.1

[b] The root-mean-square (rms) surface roughness was determined by atomic force microscopy

measured on a $3 \times 3$ μ m area.
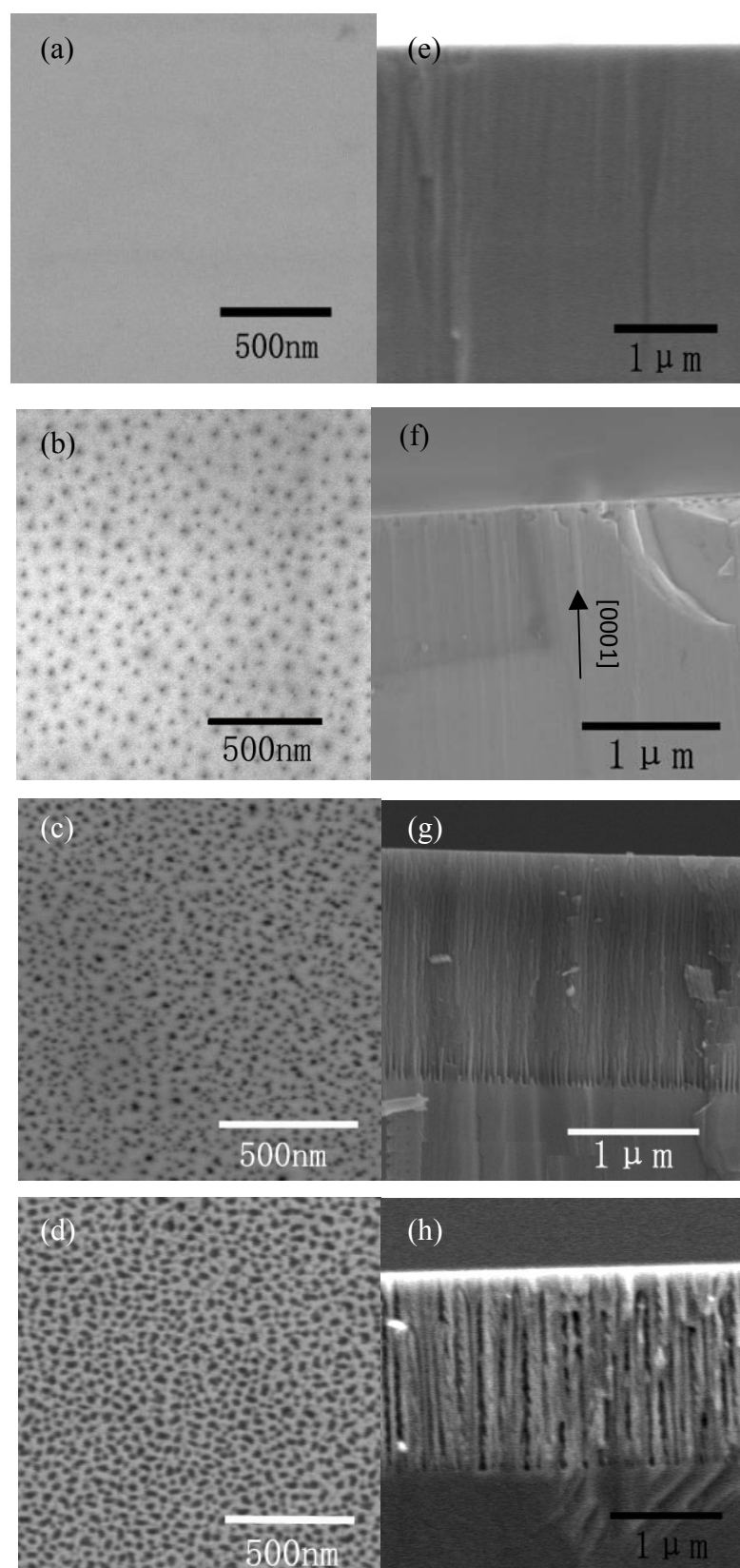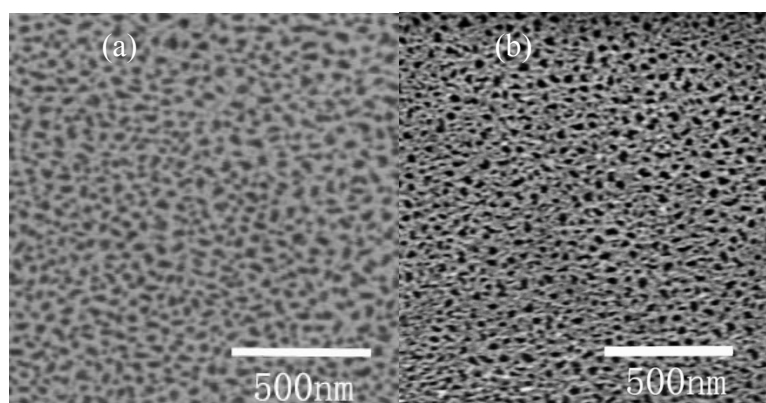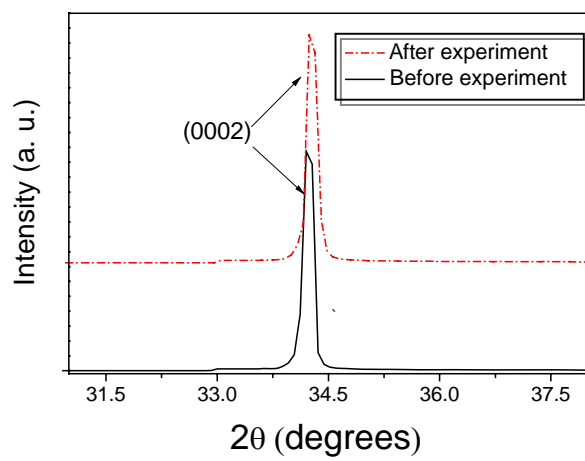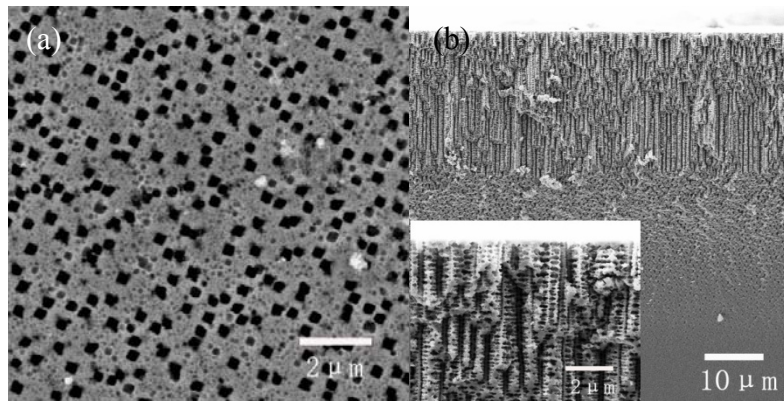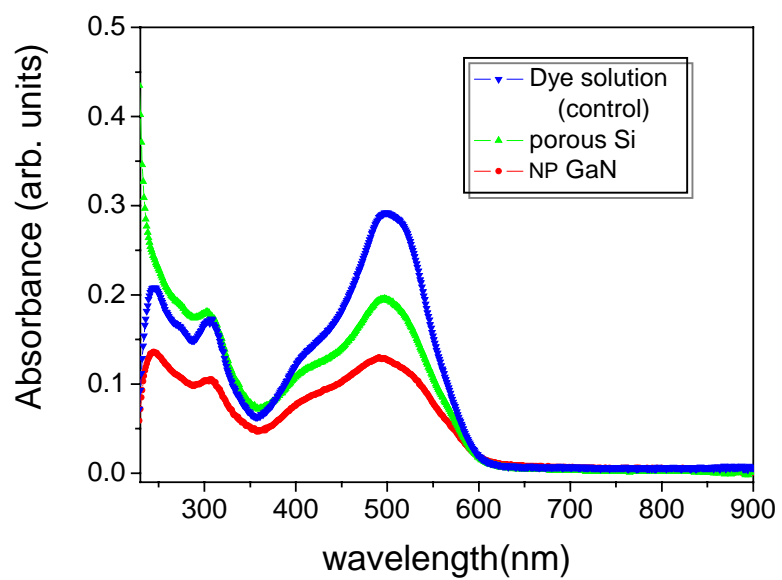
Figure 1

Figure 2
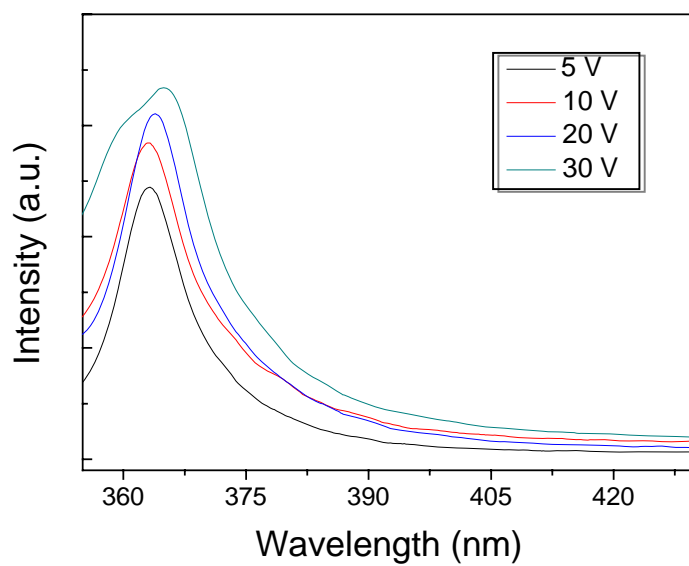
Figure 3
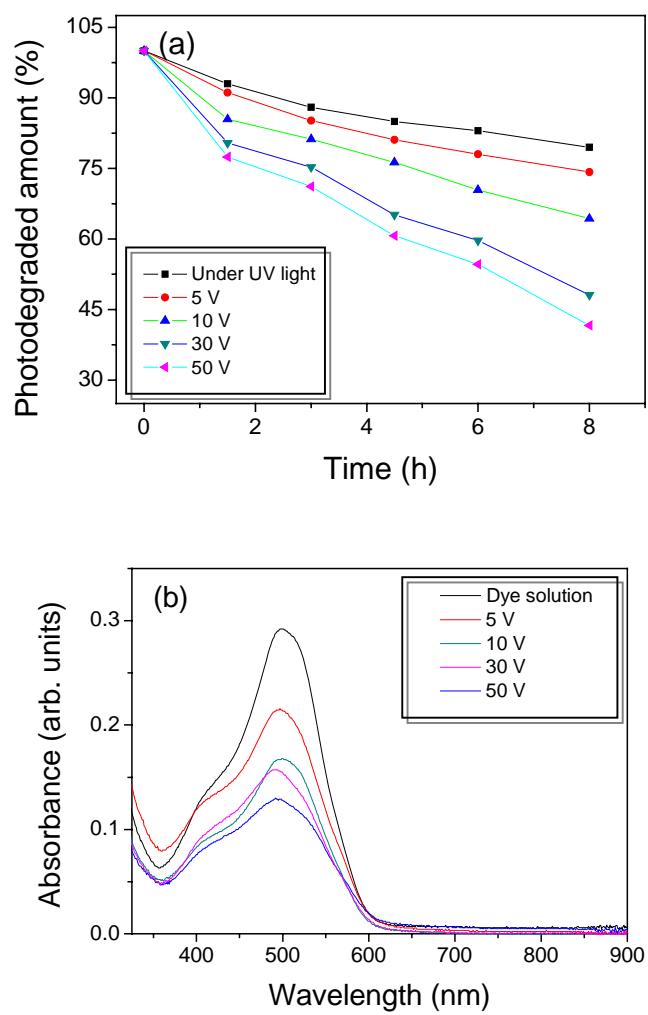
Figure 4
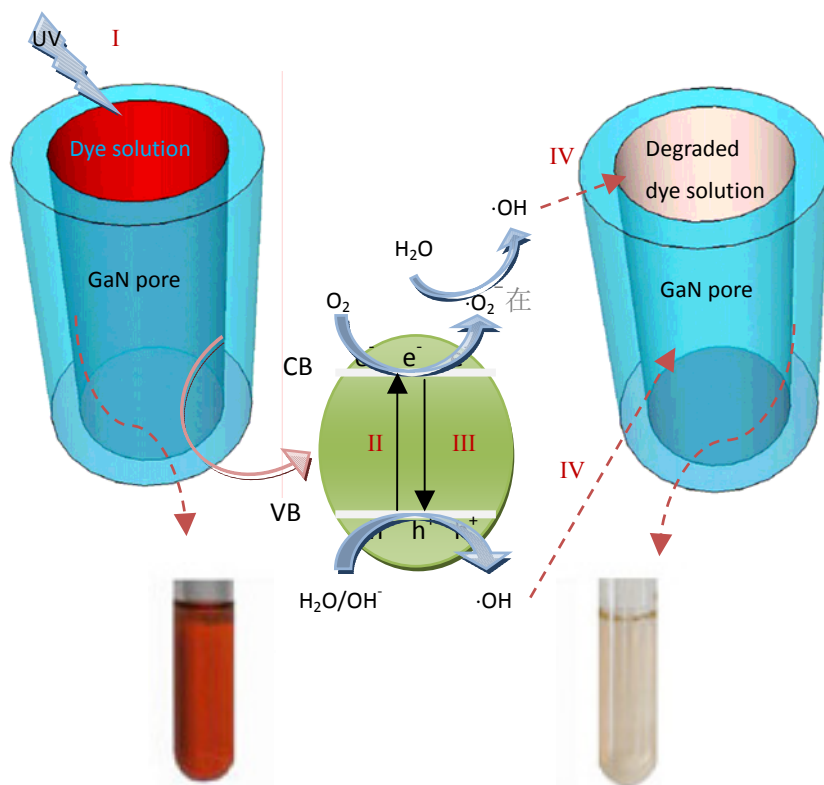
Figure 5
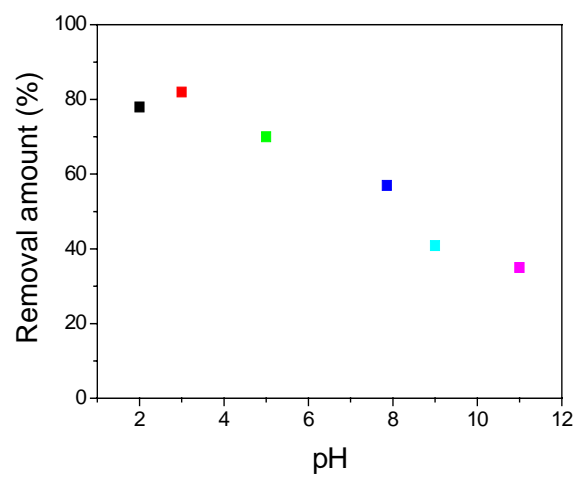
Figure 6

Figure 7

Figure8

Figure 9

**Figure 10**